ACS APPLIED MATERIALS & INTERFACES

Research Article

www.acsami.org

Highly Tunable Electrical Properties in Undoped ZnO Grown by Plasma Enhanced Thermal-Atomic Layer Deposition

M. A. Thomas[†,‡] and J. B. Cui*[,†]

[†]Department of Physics and Astronomy and [‡]Department of Applied Science, University of Arkansas at Little Rock, Little Rock, Arkansas 72204, United States

ABSTRACT: Undoped ZnO thin films with highly tunable physical properties have been achieved by a new plasma enhanced thermal atomic layer deposition. This innovative yet straightforward approach has not been reported before but is demonstrated to be capable of controlling material properties in a wide range. The structural, electrical, and optical properties of the ZnO films were investigated by various characterization techniques. The growth mechanisms are discussed in terms of the chemistry of the additional O_2 plasma on ZnO formation. Without extrinsic doping, the resistivity and carrier concentration of the ZnO films can be controlled up to seven and five orders of magnitude, respectively, by simply adjusting the plasma conditions. The electrical properties of the ZnO films were also found to correlate with significant changes in their optical properties. This extreme control and tunability of material properties is rarely achievable for undoped and even doped ZnO and should enhance the viability of ZnO in advanced device applications.

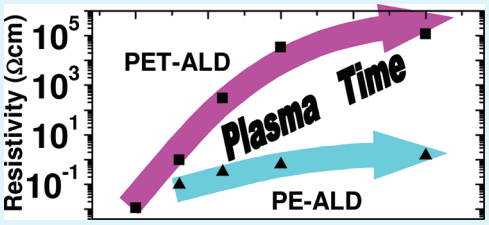

KEYWORDS: *ZnO, atomic layer deposition, plasma enhanced, resistivity, thin film transistors*

I. INTRODUCTION

The rich optical and electrical behavior of ZnO materials makes them amply suited for a range of electronic and optoelectronic device applications such as thin film transistors (TFTs), solar cells, light emitting diodes, and photodiodes.[1,2] As a result, the ability to readily tune the conductivity, charge carrier concentration, and other material properties of ZnO is highly desirable. ZnO can be obtained by a wide variety of growth methods[1,3] but controlled modulation of its useful physical properties in a single deposition process is rarely achieved. Certainly, doping of ZnO can be utilized to change its material properties, but doping can be difficult to control and reproduce and typically requires modified source materials. The deposition of undoped ZnO is therefore more straightforward, but the attributes of undoped ZnO are often preset, unflexible, and determined by the nature of the deposition technique. As an example, it has proven difficult to obtain undoped ZnO films with a wide range of electrical properties using traditional atomic layer deposition (ALD) methods.[4−6]

ALD has been established as an excellent method for the deposition of precise and uniform oxide layers in electronic devices.[7−10] Often such oxide materials are obtained by thermal-ALD processes in which H_2O vapor serves as the oxidant. In comparison to thermal-ALD techniques, the use of a plasma in ALD processes (plasma-enhanced ALD, PE-ALD) has recently shown the ability to increase the number and types of materials obtainable by ALD, lower the deposition temperature for some materials, and enhance the useful properties of ALD films for device applications.[11] In light of the increased process control in PE-ALD methods, several studies have focused on identifying the key distinctions between the established thermal-ALD and newer PE-ALD techniques for the same material, e.g., Al_2O_3,[12] TiO_2,[13] HfO_2,[14] and ZnO.[15]

In the case of ZnO, it has been well established that the dominant parameter affecting its various properties in ALD is the growth temperature. Several studies of thermal-ALD processes where H_2O is the oxidant have found that the conductivity of ZnO films can decrease by nearly three orders of magnitude as the growth temperature is lowered from 200 to 100 °C.[6,9,16] Even so, it has proven difficult to obtain high quality, "intrinsic" ZnO films with low carrier concentration and high mobility using traditional thermal-ALD methods. In situ N-doping,[5,17−19] PE-ALD,[15,20−22] spatial-ALD,[23,24] and very low growth temperatures[4,6,21,25] can, however, provide some control of ALD ZnO's properties. ALD ZnO from such methods has been used for TFT applications,[4,5,15,17−19,22] improved solar cell performance,[25] and photodiode operation.[26] Very recently, hydrogen plasma doping was utilized to control the electrical properties of PE-ALD ZnO films[27] indicating in situ plasma treatments are also an effective way to enhance ALD processes. Nevertheless, lower ALD growth temperatures and/or extrinsic doping may not provide[15,17,19] the best route toward high quality ZnO for optimal performance in device applications.

In this work, we have achieved high tunability of the material properties in *undoped* ZnO with a plasma enhanced thermal-ALD (PET-ALD) technique. In this PET-ALD approach, an in situ O_2 plasma step is added after each thermal-ALD cycle involving the standard diethylzinc (DEZ) and H_2O sequence.

Received: March 14, 2012
Accepted: May 11, 2012
Published: May 11, 2012

The as grown ZnO films have shown tunable resistivities within seven orders of magnitude, in conjunction with significant changes in their optical properties. The results are discussed in terms of the distinct oxidation pathways present in the PET-ALD process as well as the effects of the O_2 plasma on native defect and impurity formation in ZnO. Such a precise control of ZnO's properties and functionalities over a wide range without extrinsic doping has proved difficult to achieve previously.

II. EXPERIMENTAL SECTION

A. ZnO Thin Film Deposition by ALD. All ZnO thin films were prepared using a Fiji 200 ALD system from Cambridge Nanotech. The Zn precursor used in all depositions was DEZ. The PET-ALD process was established by adding an O_2 plasma step after each thermal-ALD cycle involving the standard DEZ and H_2O sequence. A remote O_2 plasma (inductively coupled, 13.56 MHz) served as the second oxidizing source. A thermal-ALD sample with no O_2 plasma treatment during growth as well as PE-ALD samples were also deposited to serve as references for comparison. The growth temperature for all the ZnO films was 200 °C. The specific details for one growth cycle in each of the ALD methods are given in Table 1.

Table 1. Process Details for One Growth Cycle in the Three Different ALD Methods Used in This Study

	ALD growth conditions (1 cycle, all depositions at 200 °C)					
process	DEZ pulse (s)	DEZ purge (s)	H_2O pulse (s)	H_2O purge (s)	O_2 plasma time (s)	O_2 plasma purge (s)
thermal-ALD	0.06	10	0.06	10	0	
PE-ALD	0.06	10			3, 6, 10, 20	5
PET-ALD	0.06	10	0.06	10	3, 6, 10, 20	5

High purity Ar was used as the process gas at a background pressure of 270−280 mTorr. This served as the working pressure during all purge steps in all of the ALD processes. All O_2 plasma steps involved a high purity O_2 flow rate of 30 sccm and plasma power of 300 W unless indicated otherwise. During the plasma steps, the working pressure in the reactor increased by ∼40 mTorr. The growth rates of the ZnO films were dependent on the type of ALD process and parameters used; however, the target thickness for the films was 50 nm. The films were deposited on both glass and Si (100) substrates.

B. ZnO Thin Film Characterization. The morphologies of the ZnO films were observed with scanning electron microscopy (SEM, JEOL JSM7000F at 15 and 30 kV). The optical properties were studied with photoluminescence (PL) utilizing the 325 nm line of a He−Cd laser and a Horiba Jobin Yvon 320 spectrometer coupled to a CCD detector. The composition of the films was analyzed with energy-dispersive X-ray spectroscopy (EDX) and X-ray photoelectron spectroscopy (XPS). The electrical properties of the ZnO films were measured with resistivity and Hall effect measurements in the van der Pauw configuration on glass substrates. Contacts were made by soldering indium metal in the corners for some of the less conductive films. The Hall effect data were taken under a magnetic field of 11.3 kG using a homemade system which includes a Keithley 7065 Hall effect card and Keithley 6220 sourcemeter.

III. RESULTS

A. Growth Rate and Structural Properties. Figure 1 displays the ZnO growth rates for the ALD processes used here. The PET-ALD process produces a growth rate of ∼1.5 Å/cycle for different O_2 plasma times, which is similar to thermal-ALD ZnO in this work (plasma time = 0 s) or previous studies.[15,28] On the other hand, the growth rate in the PE-ALD process is quite sensitive to the O_2 plasma, increasing from 0.6 to 1.1 Å/cycle as the plasma time is changed from 3 to 20 s. From the growth rate data, it is evident the ZnO growth process and reaction dynamics are distinctly changed for the PE-ALD method as compared to the PET-ALD process. In the PE-ALD process, the complete effects of the oxygen plasma on the film growth did not occur until an O_2 plasma time of ∼20 s. The constant growth rate of the PET-ALD films implies that the ZnO growth process was already completed during the thermal cycle. It should be noted that other PE-ALD studies of ZnO have typically found higher growth rates than those observed here, possibly due to the use of a "direct plasma".[12,27,29] In the direct plasma configuration, the substrate rests on one of the electrodes used to create the plasma, often producing a plasma very near the growing film surface rather than remotely as in our process. Nevertheless, in some reports of PE-ALD ZnO using a remote plasma, the observed growth rate was also significantly higher.[15,30] This suggests exact reactor designs and growth conditions can lead to distinctions in ALD processes involving a plasma. As a further comparison, another ZnO thin film was deposited in which a 15 s O_2 plasma served as the initial oxidation, followed by the normal H_2O pulse and purge *after* the plasma to complete the growth cycle. Interestingly, this film exhibited an increased growth rate of 1.2 Å/cycle in comparison to all PE-ALD samples. This indicates the extra H_2O pulse did lead to enhanced ZnO growth, providing further evidence the H_2O pulse oxidation and growth mechanism are distinct from the O_2 plasma.

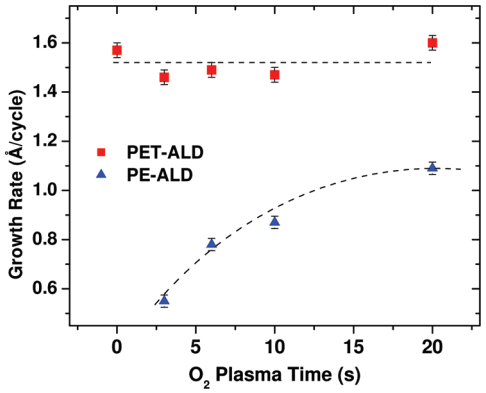

Figure 1. ZnO growth rate vs O_2 plasma time for PE-ALD and PET-ALD processes. The dashed curves are a guide for the eye.

SEM images of the ALD ZnO films are shown in Figure 2. Though the very small scale morphologies of the various films are distinct, they are all highly uniform and maintain low surface roughness, as is typical for ALD ZnO films.[21,28] The PE-ALD ZnO film's surface is made up of very small nanocrystals which are mostly vertically oriented. We did not observe any significant change in the morphology of the PE-ALD films with increasing plasma time. The two PET-ALD films have morphologies slightly in between the PE-ALD samples and the thermal-ALD film. The PET-ALD film grown with a 6 s O_2 plasma is only partially changed from the thermal-ALD sample while the 20 s PET-ALD sample possesses a surface structure closer to the PE-ALD film with oriented crystals of a much smaller average size. It is evident that the O_2 plasma leads to a surface with smaller crystals that are more vertically oriented, and as the plasma time is increased, the PET-ALD films approach the morphology and structure of the PE-ALD films.

B. Electrical Properties. Figure 3 displays the measured resistivity values for the PE-ALD and PET-ALD ZnO films.

dx.doi.org/10.1021/am300458q | ACS Appl. Mater. Interfaces 2012, 4, 3122−3128

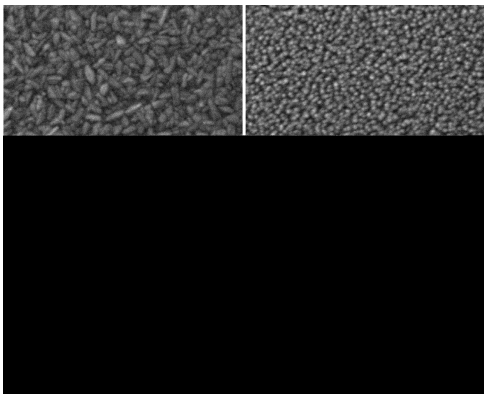

Figure 2. SEM images of ALD ZnO films: (a) thermal-ALD, (b) 6 s PE-ALD, (c) 6 s PET-ALD, and (d) 20 s PET-ALD. The scale bar in each figure is 100 nm.

Figure 3. Resistivity vs O_2 plasma time for PE-ALD and PET-ALD ZnO films.

The use of an O_2 plasma in the ALD growth process produced ZnO films with quite distinct electrical properties from what is typically achievable in thermal-ALD. The PE-ALD samples are all less conductive than the thermal-ALD reference film, consistent with results from previous studies of PE-ALD ZnO.[15,21] The PE-ALD films in this work have a range of resistivities from 0.1 to 1.5 Ω·cm, with a continuous increase in the resistivity as the O_2 plasma time is increased. Similar to the PE-ALD films, there is a continuous increase in the resistivity of the PET-ALD samples as the plasma time is also increased. However, the magnitude of the change in resistivity of the ZnO films is significantly amplified in the PET-ALD process. Whereas the thermal-ALD film has a resistivity of 1.2×10^{-2} Ω·cm, the PET-ALD sample with a 20 s plasma time is seven orders of magnitude less conductive with a resistivity of 1.2×10^{5} Ω·cm.

To explore in more detail the changes in the electrical properties of the ZnO films, their carrier concentration and mobility values are shown in Figure 4. All ALD ZnO films in this study, regardless of the growth process, were found to be *n*-type. The electron mobility does not change significantly as the plasma time is increased in the PE-ALD samples, showcasing values from 7 to 9 $cm^2/V{\cdot}s$. These mobilities are lower by a factor of three or so in comparison to the thermal-ALD sample. The structural properties of the ALD ZnO films likely play a role in the observed change in mobility. The thermal-ALD sample possessed a surface morphology with the largest crystal structures (Figure 2a), while the PE-ALD films all show very small crystals on their surface, likely leading to more grain boundaries. In polycrystalline films with moderate carrier concentrations, scattering at grain boundaries is expected to be a significant contribution to reducing carrier mobility.[31] Since the mobility of the PE-ALD samples is not drastically changed, their decreased conductivity is associated with a change in electron concentration from 8.4×10^{18} to 5.1×10^{17} cm^{-3} as the plasma time is increased from 3 to 20 s.

Figure 4. Mobility and carrier concentration vs O_2 plasma time for (a) PE-ALD and (b) PET-ALD ZnO thin films. The ∗ in (b) represents the carrier concentration of a 6 s PET-ALD film deposited using a nitrogen, rather than oxygen, plasma.

The mobility and carrier concentration of the PET-ALD ZnO films are quite strongly affected by the O_2 plasma. Even the shortest plasma time of 3 s causes the mobility of the PET-ALD films to decrease from 29 to 4 $cm^2/V{\cdot}s$, and longer plasma exposures continue to reduce the mobility. Considering the more comparable surface morphologies of the thermal-ALD and PET-ALD films (shorter plasma times), the decrease in mobility could be related to additional factors besides structural properties. This topic will be addressed further in the Discussion section. The most interesting feature of the Hall effect data for the PET-ALD films is the sequential decrease in the electron concentration as the plasma time is increased. The thermal-ALD film deposited without any plasma treatment has an electron concentration of 1.9×10^{19} cm^{-3}, while a 10 s plasma treatment after each H_2O half cycle reduces the carrier concentration to $\sim 2 \times 10^{14}$ cm^{-3}. A Hall signal could not be reliably measured for the 20 s PET-ALD film due to its high resistivity and low mobility, but on the basis of the trend with increasing plasma time, it may possess an even lower carrier concentration. A similar PET-ALD ZnO film was also deposited using a 6 s *nitrogen* plasma (asterisk in Figure 4b). This sample only displayed a slight change in carrier

concentration to 6.0×10^{18} cm^{-3} as compared to 1.8×10^{16} cm^{-3} for the 6 s O_2 plasma film. This indicates the decreased carrier concentration is strongly associated with the presence of oxygen in the plasma.

The effects of the plasma power in the PET-ALD growth process were also tested. At a 5 s plasma time, even a lower plasma power of 100 W reduces the carrier concentration significantly (1.6×10^{17} cm^{-3}) compared to the thermal-ALD reference sample, leading to an increased resistivity. As the plasma power is increased from 100 to 300 W, the carrier concentration is reduced and resistivity is increased in a nearly linear fashion. Interestingly, there is not a strong effect of the plasma power on the mobility of the PET-ALD samples, as each plasma power produced films with mobilities of ~2 cm^2/V·s.

C. Compositional Analysis. An increase in the relative oxygen content due to the O_2 plasma was observed in both ALD processes used here as measured by both EDX and XPS. In the PET-ALD films, the oxygen content increases only slightly (<1 atomic %) as the plasma time is increased. On the other hand, a rapid increase (~2 atomic %) in oxygen content occurs in the PE-ALD samples for short plasma times (up to 6 s) and then stays approximately constant afterwards. It is evident the O_2 plasma increases the oxygen content in both ALD methods; however, the effect is much stronger in the PE-ALD process because the plasma is the only oxidation pathway. These results are similar to the growth rate data discussed above.

Detailed XPS analysis of the O 1s region for selected ALD ZnO films is shown in Figure 5. Two peaks were needed to fit the O 1s regions well in all of the samples, but the peak positions and relative intensities are strongly dependent on the ALD growth conditions. The main oxygen peak in all of the samples is from the Zn−O bond in ZnO at a binding energy of 530.2−530.4 eV.[32−35] The secondary oxygen peak at ~532 eV may be from Zn−OH bonds,[32,34,35] oxygen interstitial (O_2^{2-}) type defects,[32,35] or both. For longer O_2 plasma times during growth, the main peak position was found to shift slightly to lower binding energies and the relative intensity of the secondary peak at 532 eV increases. In addition, the relative increase in oxygen content of the ZnO films compares well with the increase in the relative contribution of the 532 eV peak. These observations suggest the O_2 plasma during growth produces two effects: (1) a less "Zn heavy" bond in ZnO and (2) an increased oxygen content that is at least partially related to the secondary oxygen species at 532 eV.

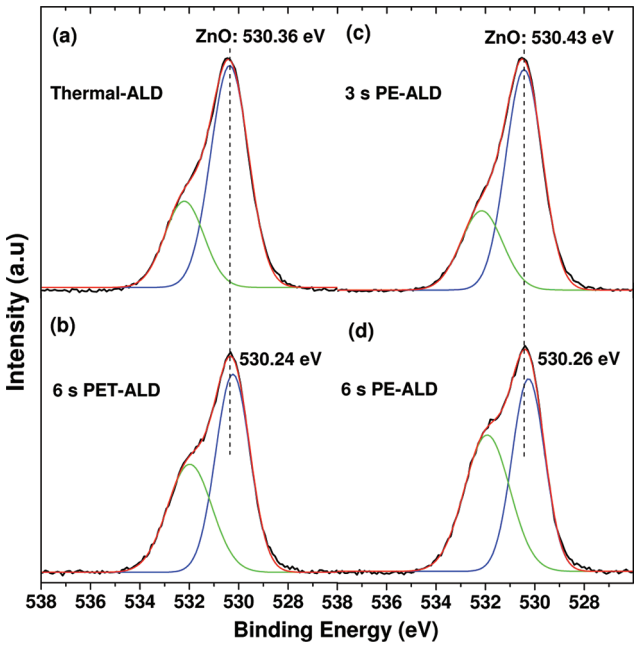

Figure 5. XPS spectra of the O 1s region for (a) thermal-ALD, (b) 6 s PET-ALD, (c) 3 s PE-ALD, and (d) 6 s PE-ALD ZnO films. The fitted peak positions for the Zn−O bond in ZnO are indicated in the figure.

The binding energy of the secondary oxygen peak in the XPS spectra is in line with expectations for Zn−OH as well as oxygen interstitial defects. ZnO films deposited by ALD using O_2 gas as the only oxidant were found to possess a completely distinct secondary oxygen species in XPS studies, different from Zn−OH found in thermal-ALD films.[32] Along this line, the relatively low intensity 532 eV binding energy peak in the thermal-ALD sample in this work is likely from Zn−OH bonds. On the other hand, the 6 s PET-ALD sample maintains a stronger 532 eV peak intensity. The only difference in the growth processes for the thermal-ALD and 6 s PET-ALD samples is the additional O_2 plasma step, so oxygen interstitial defects may be more responsible for the change in the O 1s peak contributions. The same argument holds for the PE-ALD samples. These oxygen interstitial defects are likely interpreted as oxygen trapped at grain boundaries,[36] which on the basis of the SEM images discussed previously should be expected to increase in the PE-ALD and PET-ALD ZnO films. Nevertheless, it is possible that both species are contributing to the 532 eV peak in our films as we did not find a consistent change in binding energy like in the study by Janocha and Pettenkofer.[32]

IV. DISCUSSION

A. Growth Mechanisms. The pronounced effect of the O_2 plasma on the structural, electrical, and composition properties of the ALD ZnO films may be related to its effects on their growth mechanisms. In both ALD methods used here, a O−Zn−C_2H_5 bonded structure remains on the growing film surface after each DEZ pulse.[6,16,37] In the PET-ALD process, initial oxidation of the newly formed Zn−C_2H_5 ligand occurs via a reaction with H_2O, producing ethane and leaving behind a Zn−OH surface prior to the additional O_2 plasma step.[6,16,37] In the PE-ALD growth process, an alternative oxidation pathway likely occurs. Energetic O radicals in the O_2 plasma cleave/combust the −C_2H_5 ligand bonded to Zn and subsequently oxidize Zn.[38,39] As a result, the mechanism of oxidation and Zn−O bond formation is very different in the two ALD methods. Nevertheless, there is convincing evidence an eventual (−OH) terminated surface is still formed in PE-ALD processes for oxides,[40,41] just like in thermal-ALD.

By assessing the growth rate data for the various ZnO films studied here; however, it is evident that the level of Zn−O bond formation, oxidation, and film growth are not the same when only the O_2 plasma is used as an oxidant. The decreased growth rate of the PE-ALD ZnO films implies the number of (−OH) surface sites created by each O_2 plasma cycle is lower than that established by H_2O in the thermal- or PET-ALD processes.[38,39] However, the PE-ALD ZnO films are less conductive with lower carrier concentrations than the thermal-ALD sample, especially those with a closer growth rate to the thermal-ALD film. These ideas suggest that even though the number of Zn−O bonds formed per cycle may be lower in the

dx.doi.org/10.1021/am300458q | ACS Appl. Mater. Interfaces 2012, 4, 3122−3128

PE-ALD process, the mechanism and degree of oxidation is likely improved due to the more energetic oxidation pathway associated with the O_2 plasma. Consequently, the additional plasma exposure produces a pronounced effect on the PET-ALD films' properties because Zn has already been initially oxidized by the H_2O half cycle reaction. The effects of the O_2 plasma on the structural and electrical properties of the ZnO films are then seen more readily and more significantly in the PET-ALD process as compared to PE-ALD.

B. Native Defects and Hydrogen. The conventional wisdom for ZnO is that its intrinsic conductivity is at least partially controlled by native defect concentrations.[1,42−45] Therefore, the distinctions in the ZnO films based on the growth process and plasma time may be explained by native zinc and oxygen related defects. For ALD ZnO films in particular, the enhanced *n*-type conductivity associated with thermal-ALD processes may result from several factors. An often cited source is oxygen vacancies (V_O);[9,25] however, a consensus on whether or not V_O can provide for significant *n*-type conductivity in ZnO has not been reached.[44−46] Zn interstitials (Zn_i) on the other hand are generally agreed to be more directly involved with the native *n*-type conductivity in ZnO[42,44,45] and therefore may play a larger role in establishing the high electron concentrations in thermal-ALD.

Another explanation for the *n*-type conductivity in ZnO that has been well established by both experiment[47,48] and theory[49,50] is hydrogen impurities. Certainly, hydrogen is present in ALD processes for ZnO as both DEZ and H_2O contain hydrogen and a Zn−OH bond is produced every half cycle. The fact that PE-ALD ZnO, which does not utilize H_2O, consistently shows lower *n*-type conductivity than thermal-ALD ZnO suggests hydrogen may play a role. A potential explanation is that hydrogen is present in ZnO by any ALD process, but when an O_2 plasma is used as in PE-ALD or PET-ALD, it can effectively remove hydrogen impurities. Such behavior has been directly observed before when chemical vapor deposited (CVD) ZnO films were treated "ex-situ" with an H_2 plasma and then an O_2 plasma.[51] It was suggested that hydrogen has particularly rich and varied behavior in polycrystalline ZnO films due to its accumulation at grain boundaries, but an O_2 plasma is capable of reducing its presence, especially at slightly elevated temperatures (225 °C).[51] This may help to explain the distinct effect of the O_2 plasma in the PET-ALD process used here, in particular because the plasma treatment is in situ and occurs every growth cycle. It is worth noting though that some studies of ALD ZnO have shown reduced *n*-type conductivities in ZnO actually trend with an increase in measured hydrogen content.[4,25] This is explained in terms of a larger number of (−OH) related defects that both increase the hydrogen content and reduce the electron concentration.[4] Recall that both the PE-ALD and PET-ALD ZnO films studied here showed a possible increase in Zn−OH related bonds by XPS.

The use of an O_2 plasma to reduce the inherent *n*-type conductivity in ZnO has been explored in other growth methods such as molecular beam epitaxy[52,53] and pulsed laser deposition.[54] Similarly, very resistive ZnO materials can be fabricated by increasing the oxygen partial pressure in sputtering processes.[55] Indeed, Min et al. recently tested a similar idea to this work where ozone gas was added after the normal DEZ-H_2O thermal-ALD cycle and found that the ozone treatment reduced the background electron concentration of the ZnO films.[56] There is little argument that more oxygen-rich ZnO should trend toward lower electron concentrations and higher resistivities. However, a decreased electron concentration can in principle be created by reducing the number of donor defects or increasing acceptor or trap defects. Since the mobilities of the PE-ALD and PET-ALD ZnO films in this study do not significantly increase along with the decrease in free carriers, the changes in carrier concentration may also be related to compensating acceptors or charge traps created by the longer O_2 plasma exposure. This idea is supported and discussed in detail below with regard to connections between changes in the optical, electrical, and composition properties of the ALD ZnO films due to the O_2 plasma.

C. Correlation between Optical and Electrical Properties. The distinct changes in the electrical properties of the ALD ZnO films were also found to correlate with their optical properties. Room temperature PL was measured for the ZnO films and is shown in Figure 6a. The defect PL emissions are in the yellow/orange and red portion of the spectrum (≤2.3 eV), quite distinct from the "green band" typically observed in ZnO.[1,57] The relative intensities of the near band edge (NBE) and defect emissions depend on the plasma treatment in the ALD processes. A longer O_2 plasma time creates a stronger defect PL contribution in the ZnO films. The defect/NBE intensity ratio is often used as a measure of the defect density in ZnO.[1,57] In Figure 6b, a consistent trend can be seen in both growth processes that the samples with larger defect/NBE intensity ratios also maintain a lower carrier concentration. Such an observation seems to indicate that the presence of defects in ZnO causes its carrier concentration to decrease, which may be an unexpected relationship.[42−45] Furthermore, the carrier concentrations in the PET-ALD films show a much stronger dependence on the defect presence than the PE-ALD samples. This helps to illustrate the more prominent influence of the O_2 plasma in the PET-ALD process. Other studies of both thermal-ALD[28] and PE-ALD ZnO[15] have shown that films deposited at low growth temperatures maintained increased defect PL emissions along with reduced electron concentrations.

The two defect emissions at 1.8 and 2.1 eV are not especially common, but they have been previously observed in ZnO materials and are often associated with excess oxygen in general. Polycrystalline Ga-doped ZnO films were shown to possess a PL band at 1.8 eV in connection with compensating zinc vacancies (V_{Zn}) that spontaneously form due to the high level of *n*-type doping.[58] A 2.1 eV PL peak was also found to increase consistently with remote oxygen plasma treatment time of Zn-face bulk ZnO.[59] The oxygen plasma treatment reduced the electron concentration in these bulk ZnO samples as well, allowing for improved Schottky contact formation. The authors suggested their results were best explained by the 2.1 eV band originating from a native defect acting as a compensating acceptor, possibly V_{Zn}.[59] These results are similar to those discussed above where CVD ZnO films were treated with H_2 and O_2 plasmas. In that study, the authors provided a related mechanism in that the O_2 plasma reacts with hydrogen passivating V_{Zn} sites to produce H_2O and an active V_{Zn}.[51] This idea may be strengthened by the fact that the thermal-ALD and 3 s PE-ALD films in this work possess strong NBE luminescence along with minimal defect emissions and also have the highest *n*-type conductivity. Many studies associated with various hydrogen treatments of ZnO have indicated NBE luminescence is enhanced and defect emissions are reduced due to hydrogen's ability to passivate native defects.[60−62] The

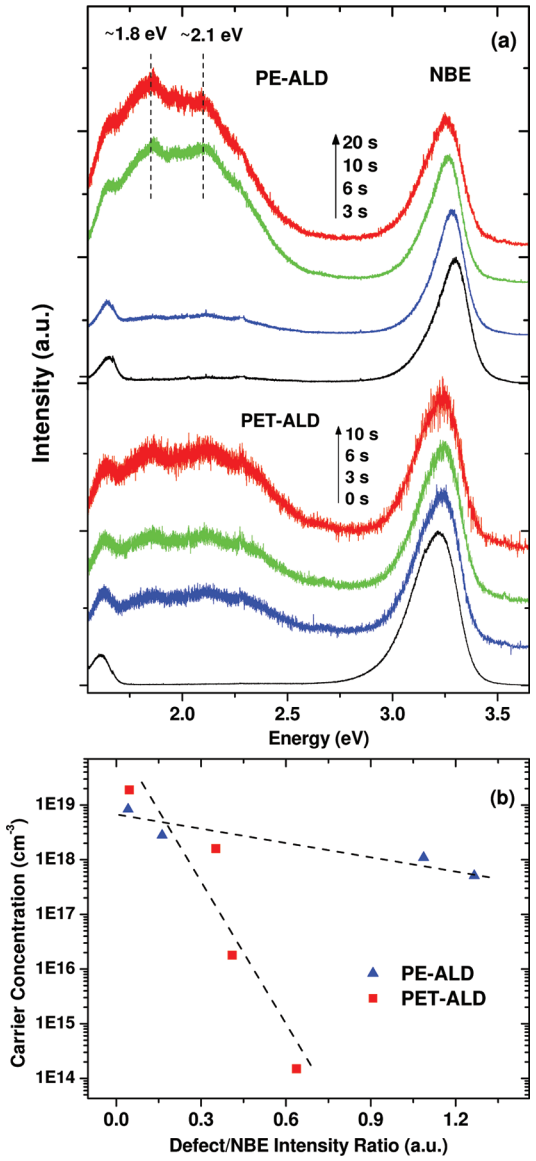

Figure 6. (a) PL spectra of ALD ZnO films grown with different O_2 plasma times as indicated in the figure (0 s = thermal-ALD). The spectra have been normalized to the NBE emission intensity and are offset vertically for clarity. (b) Carrier concentration vs defect/NBE intensity ratio for PE-ALD and PET-ALD ZnO samples. The dashed lines are simply guides for the eye.

opposite PL trends with increasing O_2 plasma time seen in this work lend credence to the idea that the plasma in fact removes hydrogen from ZnO. The innate presence of V_{Zn} in ALD ZnO films might be expected from incomplete surface saturation of DEZ.[63] These "open" surface sites have in fact been exploited to improve the Al doping uniformity in Al-doped ZnO films by ALD.[64] Regardless of the specific mechanism, the experimental results seem to indicate that O_2 plasma treatments increase the concentration of V_{Zn} or other native defects in ZnO, leading to reduced electron concentrations.

D. Summary. Considering all the results discussed to this point, the O_2 plasma likely plays several roles in the ALD growth process. First, it helps to completely oxidize Zn during each plasma step in the growth cycle, potentially filling in V_O and eliminating Zn_i that may play a role in the native *n*-type conductivity in ZnO.[42−45] Since Zn_i defects are expected to be quite mobile at the 200 °C growth temperature used here,[45] they may be effectively removed by their reaction with the O_2 plasma to form ZnO on the film surface. Evidence for the increased oxidation was found in the growth rate data, electrical properties, and compositional analysis of the ZnO films. Second, the plasma produces ZnO films with much smaller average crystallites, likely leading to more grain boundaries and the potential for related defects. Third, in addition to creating a more balanced Zn−O bond, the O_2 plasma establishes new oxygen species in the growing ZnO films which may be linked to interstitial oxygen at grain boundaries[32,36] or (−OH) defects.[4] The SEM images and XPS analysis of the films provided strong support for these ideas. Finally, the inherent presence of hydrogen in ALD processes and its role in the *n*-type conductivity in ZnO materials suggest the O_2 plasma is also effective in removing hydrogen. This idea could pertain to both electrically active hydrogen impurities as well as hydrogen passivators occupying native defect sites. Overall, the increased oxidation, formation of compensating acceptor defects, and removal of hydrogen are expected to reduce the native *n*-type character and increase the resistivity of ZnO, which is indeed observed here.

The results associated with the changes in the physical properties of the various ALD ZnO films are potentially interesting for the purpose of tuning the conductivity and carrier concentration in ZnO. By simply combining the classic thermal-ALD growth process with an O_2 plasma, it is possible to control the electrical properties of ZnO within a very wide range. Previously, such low carrier concentrations and high resistivities have mainly been achieved in ALD ZnO by utilizing low growth temperatures and extrinsic doping.[5,17,19] The reliable, straightforward, and expansive control of ZnO's electrical properties achieved in this work is rare in ZnO deposition without extrinsic doping. In addition, considering ALD's potential to uniformly coat practically any structure or morphology,[65] the capability to modulate its electrical behavior should serve as an important step in improving advanced device applications utilizing 3D nanomaterials, as evidenced in a recent report on ALD ZnO/Si nanowire photodiodes.[26] The combination of thermal and plasma growth mechanisms in the PET-ALD technique may also create the opportunity to improve the useful properties of other material systems in ALD processes.

V. CONCLUSION

A new plasma enhanced thermal-ALD (PET-ALD) process has been developed to grow ZnO thin films. An O_2 plasma was introduced after the oxidation by H_2O vapor to establish the PET-ALD growth, enabling highly tunable electrical properties of undoped ZnO thin films. The ability to reliably control the resistivity of ZnO up to seven orders of magnitude without extrinsic doping is unprecedented and important for potential device applications such as thin film transistors with desirable functionalities. While the growth mechanism needs to be explored further, this new PET-ALD approach may be extended to other material systems for improved property control.

AUTHOR INFORMATION

Corresponding Author

*E-mail: jxcui@ualr.edu.

Notes

The authors declare no competing financial interest.

■ ACKNOWLEDGMENTS

This work was supported by the National Science Foundation under award No. EPS-1003970. The authors would like to thank the UALR Nanotechnology Center for use of its SEM facilities.

■ REFERENCES

(1) Ozgur, U.; Alivov, Y.I.; Liu, C.; Teke, A.; Reshchikov, M.A.; Dogan, S.; Avrutin, V.; Cho, S.J.; Morkoc, H. *J. Appl. Phys.* **2005**, *98*, 041301 , and references therein..
(2) Look, D.C. *Mat. Sci. Eng. B* **2001**, *80*, 383.
(3) Klingshirn, C. *Phys. Status Solidi B* **2007**, *244*, 3027.
(4) Huby, N; Ferrari, S.; Guziewicz, E.; Godlewski, M.; Osinniy, V. *Appl. Phys. Lett.* **2008**, *92*, 023502.
(5) Levy, D.H.; Nelson, S.F. *J. Vac. Sci. Technol., A* **2012**, *30*, 018501.
(6) Krajewski, T.; Guziewicz, E.; Godlewski, M.; Wachnicki, L.; Kowalik, I.A.; Wojcik-Glodowska, A.; Lukasiewicz, M.; Kopalko, K.; Osinniy, V.; Guziewicz, M. *Microelectron. J.* **2009**, *40*, 293.
(7) Leskela, M.; Ritala, M. *Thin Solid Films* **2002**, *409*, 138.
(8) Niinisto, L; Paivasaari, J.; Niinisto, J.; Putkonen, M.; Nieminen, M. *Phys. Status Solidi A* **2004**, *201*, 1443.
(9) Godlewski, M.; et al. *Microelectron. Eng.* **2008**, *85*, 2434.
(10) Javey, A.; Kim, H.; Brink, M.; Wang, Q.; Ural, A.; Guo, J.; McIntyre, P.; McEuen, P.; Lundstrom, M.; Dai, H.J. *Nat. Mater.* **2002**, *1*, 241.
(11) Profijt, H.B.; Potts, S.E.; van de Sanden, M.C.M.; Kessels, W.M.M. *J. Vac. Sci. Technol., A* **2011**, *29*, 050801.
(12) van Hemmen, J.L.; Heil, S.B.S.; Klootwijk, J.H.; Roozeboom, F.; Hodson, C.J.; van de Sanden, M.C.M.; Kessels, W.M.M. *J. Electrochem. Soc.* **2007**, *154*, G165.
(13) Maeng, W.J.; Kim, H. *Electrochem. Solid-State Lett.* **2006**, *9*, G191.
(14) Park, P.K.; Roh, J.S.; Choi, B.H.; Kang, S.W. *Electrochem. Solid-State Lett.* **2006**, *9*, F34.
(15) Kim, D.; Kang, H.; Kim, J.M.; Kim, H. *Appl. Surf. Sci.* **2011**, *257*, 3776.
(16) Godlewski, M.; Guziewicz, E.; Luka, G.; Krajewski, T.; Lukasiewicz, M.; Wachnicki, L.; Wachnicka, A.; Kopalko, K.; Sarem, A.; Dalati, B. *Thin Solid Films* **2009**, *518*, 1145.
(17) Lim, S.J.; Kwon, S.J.; Kim, H.; Park, J.S. *Appl. Phys. Lett.* **2007**, *91*, 183517.
(18) Levy, D.H.; Freeman, D.; Nelson, S.F.; Cowdery-Corvan, P.J.; Irving, L.M. *Appl. Phys. Lett.* **2008**, *92*, 192101.
(19) Lim, S.J.; Kim, J.M.; Kim, D.; Kwon, S.; Park, J.S.; Kim, H. *J. Electrochem. Soc.* **2010**, *157*, H214.
(20) Park, S.H.K.; Hwang, C.S.; Jeong, H.Y.; Chu, H.Y.; Cho, K.I. *Electrochem. Solid-State Lett.* **2008**, *11*, H10.
(21) Rowlette, P.C.; Allen, C.G.; Bromley, O.B.; Dubetz, A.E.; Wolden, C.A. *Chem. Vap. Deposition* **2009**, *15*, 15.
(22) Mourey, D.A.; Zhao, D.A.L.; Sun, J.; Jackson, T.N. *IEEE Trans. Electron Devices* **2010**, *57*, 530.
(23) Nelson, S.F.; Levy, D.H.; Tutt, L.W.; Burberry, M. *J. Vac. Sci. Technol., A* **2012**, *30*, 01A154.
(24) Illiberi, A.; Roozeboom, F.; Poodt, P. *ACS Appl. Mater. Interfaces* **2012**, *4*, 268.
(25) Chang, C.Y.; Tsai, F.Y. *J. Mater. Chem.* **2011**, *21*, 5710.
(26) Kang, H.; Park, J.; Choi, T.; Jung, H.; Lee, K.H.; Im, S.; Kim, H. *Appl. Phys. Lett.* **2012**, *100*, 041117.
(27) Kwon, J.D.; Lee, J.W.; Nam, K.S.; Kim, D.H.; Jeong, Y.S.; Kwon, S.H.; Park, J.S. *Curr. Appl. Phys.* **2012**, DOI: 10.1016/j.cap 2012.02.044.
(28) Guziewicz, E.; Kowalik, I.A.; Godlewski, M.; Kopalko, K.; Osinniy, V.; Wojcik, A.; Yatsuneuko, S.; Lusakowska, E.; Paszkowicz, W.; Guziewicz, M. *J. Appl. Phys.* **2008**, *103*, 033515.
(29) Park, S.H.K.; Hwang, C.S.; Kwack, H.S.; Lee, J.H.; Chu, H.Y. *Electrochem. Solid-State Lett.* **2006**, *9*, G299.
(30) Kwon, S.K.; Kim, D.W.; Jung, Y.H.; Lee, B.J. *J. Korean Phys. Soc.* **2009**, *55*, 999.
(31) Minami, T. *Semicond. Sci. Technol.* **2005**, *20*, S35.
(32) Janocha, E.; Pettenkofer, C. *Appl. Surf. Sci.* **2011**, *257*, 10031.
(33) Lupan, O; Pauporte, T; Chow, L; Viana, B; Pelle, F; Ono, L.K.; Cuenya, B.R.; Heinrich, H. *Appl. Surf. Sci.* **2010**, *256*, 1895.
(34) Tak, Y.; Park, D.; Yong, K.J. *J. Vac. Sci. Technol., B* **2006**, *24*, 2047.
(35) Bang, S.; Lee, S.; Park, J.; Park, S.; Ko, Y.; Choi, C.; Chang, H.; Park, H.; Jeon, H. *Thin Solid Films* **2011**, *519*, 8109.
(36) Kim, Y.J.; Kim., H.J. *Mater. Lett.* **1999**, *41*, 159.
(37) Elliott, S.D.; Scarel, G.; Wiemer, C.; Fanciulli, M.; Pavia, G. *Chem. Mater.* **2006**, *18*, 3764.
(38) Heil, S.B.S.; Kudlacek, P.; Langereis, E.; Engeln, R.; van de Sanden, M.C.M.; Kessels, W.M.M. *Appl. Phys. Lett.* **2006**, *89*, 131505.
(39) Heil, S.B.S.; van Hemmen, J.L.; van de Sanden, M.C.M.; Kessels, W.M.M. *J. Appl. Phys.* **2008**, *103*, 103302.
(40) Langereis, E.; Keijmel, J.; van de Sanden, M.C.M.; Kessels, W.M.M. *Appl. Phys. Lett.* **2008**, *92*, 231904.
(41) Heil, S.B.S.; Roozeboom, F.; van de Sanden, M.C.M.; Kessels, W.M.M. *J. Vac. Sci. Technol., A* **2008**, *26*, 472.
(42) Look, D.C.; Hemsky, J.W.; Sizelove, J.R. *Phys. Rev. Lett.* **1999**, *82*, 2552.
(43) Tuomisto, F.; Saarinen, K.; Look, D.C.; Farlow, G.C. *Phys. Rev. B* **2005**, *72*, 085206.
(44) Kohan, A.F.; Ceder, G.; Morgan, D.; Van de Walle, C.G. *Phys. Rev. B* **2000**, *61*, 15019.
(45) Janotti, A.; Van de Walle, C.G. *Phys. Rev. B* **2007**, *76*, 165202.
(46) Zhang, S.B.; Wei, S.H.; Zunger, A. *Phys. Rev. B* **2001**, *63*, 075205.
(47) Cox, S.F.J.; Davis, E.A.; Cottrell, S.P.; King, P.J.C.; Lord, J.S.; Gil, J.M.; Alberto, H.V.; Vilao, R.C.; Duarte, J.P.; de Campos, N.A. *Phys. Rev. Lett.* **2001**, *86*, 2601.
(48) Hofmann, D.M.; Hofstaetter, A.; Leiter, F.; Zhou, H.J.; Henecker, F.; Meyer, B.K.; Orlinskii, S.B.; Schmidt, J.; Baranov, P.G. *Phys. Rev. Lett.* **2002**, *88*, 045504.
(49) Van de Walle, C.G. *Phys. Rev. Lett.* **2000**, *85*, 1012.
(50) Janotti, A.; Van de Walle, C.G. *Nat. Mater.* **2007**, *6*, 44.
(51) Wolden, C.A.; Barnes, T.M.; Baxter, J.B.; Aydil, E.S. *J. Appl. Phys.* **2005**, *97*, 043522.
(52) Chen, Y.F.; Ho, S.K.; Ko, H.J.; Nakajima, M.; Yao, T.; Segawa, Y. *Appl. Phys. Lett.* **2000**, *76*, 245.
(53) Kato, H.; Sano, M.; Miyamoto, K; Yao, T. *Jpn. J. Appl. Phys. 2* **2003**, *42*, L1002.
(54) Gu, Y.F.; Li, X.M.; Yu, W.D.; Gao, X.D.; Zhao, J.L.; Yang, C. *J. Cryst. Growth* **2007**, *305*, 36.
(55) Carcia, P.F.; McLean, R.S.; Reilly, M.H.; Nunes, G., Jr. *Appl. Phys. Lett.* **2003**, *82*, 1117.
(56) Min, Y.S.; An, C.J.; Kim, S.K.; Song, J.; Hwang, C.S. *Bull. Korean Chem. Soc.* **2010**, *31*, 2503.
(57) Djurisic, A.B.; Leung, Y.H. *Small* **2006**, *2*, 944.
(58) Look, D.C.; Leedy, K.D.; Vines, L.; Svensson, B.G.; Zubiaga, A.; Tuomisto, F.; Doutt, D.R.; Brillson, L.J. *Phys. Rev. B* **2011**, *84*, 115202.
(59) Dong, Y.F.; Fang, Z.Q.; Look, D.C.; Doutt, D.R.; Cantwell, G.; Zhang, J.; Song, J.J.; Brillson, L.J. *J. Appl. Phys.* **2010**, *108*, 103718.
(60) Kim, M.D.; Oh, J.E.; Kim, S.G.; Yang, W.C. *Solid State. Commun.* **2011**, *151*, 768.
(61) Shi, W.S.; Agyeman, O.; Xu, C.N. *J. Appl. Phys.* **2002**, *91*, 5640.
(62) Lin, C.C.; Chen, H.P.; Liao, H.C.; Chen, S.Y. *Appl. Phys. Lett.* **2005**, *86*, 183103.
(63) Makino, H.; Miyake, A.; Yamada, T.; Yamamoto, N.; Yamamoto, T. *Thin Solid Films* **2009**, *517*, 3138.
(64) Kim, J.Y.; Choi, Y.J.; Park, H.Y.; Gulledge, S.; Johnson, D.C. *J. Vac. Sci. Technol., A* **2010**, *28*, 1111.
(65) Bae, C.D.; Shin, H.J.; Nielsch, K. *MRS Bull.* **2011**, *36*, 887.